

# Gold Nanoparticles Coated with Semi-Fluorinated Oligo(ethylene glycol) Produce Sub-100 nm Nanoparticle Vesicles without Templates

Kenichi Niikura,<sup>\*,†</sup> Naoki Iyo,<sup>‡</sup> Takeshi Higuchi,<sup>§</sup> Takashi Nishio,<sup>‡</sup> Hiroshi Jinnai,<sup>§</sup> Naoki Fujitani,<sup>||</sup> and Kuniharu Ijro<sup>†,⊥</sup>

<sup>†</sup>Research Institute for Electronic Science (RIES), Hokkaido University, Kita 21, Nishi 10, Kita-Ku, Sapporo 001-0021, Japan

<sup>‡</sup>Graduate School of Chemical Sciences and Engineering, Hokkaido University, Kita 13, Nishi 8, Kita-Ku, Sapporo 060-8628, Japan

<sup>§</sup>Institute for Materials Chemistry and Engineering (IMCE) and Japan Science and Technology Agency (JST), ERATO, Takahara Soft Interfaces Project, CE 80, Kyushu University, 744 Motooka, Nishi-ku, Fukuoka 819-0395, Japan

<sup>||</sup>Graduate School of Advanced Life Science, Frontier Research Center for Post-Genome Science and Technology, Hokkaido University, Sapporo, Japan

<sup>⊥</sup>CREST, Japan Science and Technology Agency (JST), Sanban-cho 5, Chiyoda-ku, Tokyo 102-0075, Japan

## S Supporting Information

**ABSTRACT:** Gold nanoparticles (NPs) with diameters of 5, 10, and 20 nm coated with semifluorinated oligo(ethylene glycol) ligands were formed into sub-100 nm hollow NP assemblies (NP vesicles) in THF without the use of a template. The NP vesicles maintained their structure even after the solvent was changed from THF to other solvents such as butanol or CH<sub>2</sub>Cl<sub>2</sub>. NMR analyses indicated that the fluorinated ligands are bundled on the NPs and that the solvophobic feature of the fluorinated bundles is the driving force for NP assembly. The formed NP vesicles were surface-enhanced Raman scattering-active capsules.

Interparticle plasmonic coupling in an assembly produces collective properties different from those of the dispersed particles; therefore, metal and semiconductor nanoparticle (NP) assemblies are of considerable interest in many fields, such as materials, analytical, and medical sciences.<sup>1–3</sup> The vesicular assembly of NPs (NP vesicles), in particular, will provide new applications for NPs through utilization of the inner space for drug delivery systems,<sup>4</sup> catalyst carriers, surface-enhanced Raman scattering (SERS) sensing platforms, and so on.<sup>5</sup> In particular, for drug delivery carriers, such as micelles, a diameter of <100 nm is known to be important for targeting tumor cells.<sup>6</sup> To extend such applications, a new approach to the assembly or organization of NPs must be developed. As a conventional approach for the construction of NP vesicles, templates have been often used. For example, emulsion drops, known as Pickering emulsion, have been used to assemble NPs at the liquid–liquid interface.<sup>7</sup> In many cases, the emulsion-drop-templated method gives micrometer-sized NP vesicles.<sup>8</sup> Liposomes have also been used as templates to produce NP vesicles;<sup>9</sup> however, the size of the NPs that can be embedded in lipid bilayers is limited to <6 nm, which makes plasmonic applications difficult. When template molecules are used as a

core to assemble NPs,<sup>10</sup> the inner space might not be sufficient to enclose drugs.

To utilize the cavity in NP vesicles, the development of alternative assembly approaches that do not use a template is important. Stucky and co-workers reported the one-pot synthesis of NP vesicles using polyamine and negatively charged quantum dots.<sup>11</sup> Recently, the codisplay of hydrophobic and hydrophilic ligands on the surface of NPs provided an amphiphilic feature to NPs, inducing their self-assembly.<sup>12–14</sup> Kumacheva and co-workers reported the vesicular assembly of hydrophilic cetyltrimethylammonium bromide (CTAB)-coated gold nanorods by partial modification with hydrophobic polystyrene.<sup>12</sup> The coating of gold NPs (AuNPs) with hydrophobic poly(methyl methacrylate) (PMMA) and hydrophilic poly(ethylene glycol) (PEG) has also been reported to result in the formation of NP vesicles.<sup>13</sup> However, there have been few reports of NP vesicles with sub-100 nm diameters constructed using these self-assembly approaches.

Herein we demonstrate that surface modification with a single molecule, a semifluorinated ligand (SFL), can efficiently produce sub-100 nm NP vesicles (~60 nm in diameter) in tetrahydrofuran (THF) solution. The newly synthesized SFLs were composed of three parts: oligo(ethylene glycol) (OEG), fluorinated tetraethylene glycol (FG), and an 11-carbon alkyl chain with a thiol terminus (Scheme 1). This approach is based on simple one-pot ligand modification and was found to be applicable to AuNPs with diameters of 5, 10, and 20 nm. We believe that the important feature of this work is the preparation of NP vesicles using a homogeneous small surface ligand instead of multiple different polymers as in previous reports. The coating with small molecules allows the gaps between the NPs to be significantly decreased, expanding the plasmonic application of the NP vesicles. To emphasize these merits, we demonstrate that NP vesicles can be used as a

Received: March 3, 2012

Published: April 25, 2012

**Scheme 1. Structure of the SFL Used in This Study and Self-Assembly of SFL-AuNPs to Generate NP Vesicles**


platform for optically enhanced spectroscopies such as SERS in solution because of the close packing of the NPs.

SFL-coated AuNPs (SFL-AuNPs) were synthesized through ligand exchange from citric acid to SFLs in THF. SFLs in THF (2 mM, 1 mL) were added to an aqueous solution (20  $\mu$ L) of citric acid-coated AuNPs (10 nm diameter) and purified by repeated centrifugation. The AuNP solution changed from red to purple soon after mixing of the AuNPs and SFLs, indicating that AuNP assemblies were formed in the solution. UV-vis spectral analysis showed that the surface plasmon resonance band of the NP vesicles displayed a 30 nm red shift relative to that of dispersed dodecanethiol-coated AuNPs in THF (Figure S1 in the Supporting Information), supporting our assumption that AuNP assemblies were formed in the solution. The interparticle distance was estimated to be 2.5 nm from the scanning electron microscopy (SEM) image. This interparticle distance was also supported by the shift in the plasmon peak. In the case of a 10.5 nm AuNP superlattice, a plasmon shift of 30 nm was reported for an interparticle gap of 2.3 nm,<sup>15</sup> which is in good agreement with our results. The length of the linear form of the SFL is calculated to be  $\sim$ 3.6 nm; therefore, interdigitation of the ligands should occur in the interparticle gap (see Figure 3d). The ligand coverage on a single AuNP was calculated to be 58.1% on the basis of the S/Au molar ratio

obtained by inductively coupled plasma optical emission spectroscopy (ICP-OES) (Table S1). This number corresponds to a 1:2 molecular ratio of ligands to surface Au atoms, indicating almost complete ligand coverage.<sup>16</sup> SEM showed the efficient formation of spherical assemblies of NPs (Figure 1). The average diameter of the NP vesicles as judged from the SEM images (300 counts) was 65 nm for 10 nm AuNPs, and the size distribution was relatively narrow. Dynamic light scattering measurements also confirmed this, giving an assembly size of  $\sim$ 68 nm in THF solution (Figure S2). In addition to the 10 nm AuNPs, AuNPs with diameters of 5 and 20 nm also formed NP vesicles (Figure 1c,d). The average diameter of the vesicles increased with increasing size of the NPs (60 and 95 nm for 5 and 20 nm AuNPs, respectively). Transmission electron microscopy (TEM) images indicated the characteristic hollow structures with high contrast between the shell and the interior (Figure 1e).

Transmission electron microtomography (TEMT) was used to probe the three-dimensional (3D) structure of the NP assemblies. NP vesicles made from 5 nm AuNPs were embedded in epoxy resin (Epok-812) by curing at 60  $^{\circ}$ C for 12 h. Thin-film sections of this epoxy resin were prepared using an ultramicrotome (Leica Ultracut UCT). The sections were transferred on a Cu grid with a poly(vinyl fluoride) (PVF) supporting membrane. A series of TEM images were acquired at 1 $^{\circ}$  tilt intervals from  $-73.6$  to  $75.8^{\circ}$ . The tilt-series images were aligned with a fiducial marker method using AuNPs as the fiducial markers and then reconstructed using the filtered-back-projection (FBP) method.<sup>17</sup> A series of images sliced along the XY plane for the same specimen area at various height positions are shown in Figure 2a. In these images, the spherical dark regions correspond to the AuNPs, and the assembly (indicated by the black arrow) was reconstructed. The 3D image of the assembly clearly shows the hollow spherical structures of the NP vesicles composed of a single layer of AuNPs (Figure 2b).

To clarify the mechanism of NP vesicle formation, we increased the number of terminal ethylene glycol units of the

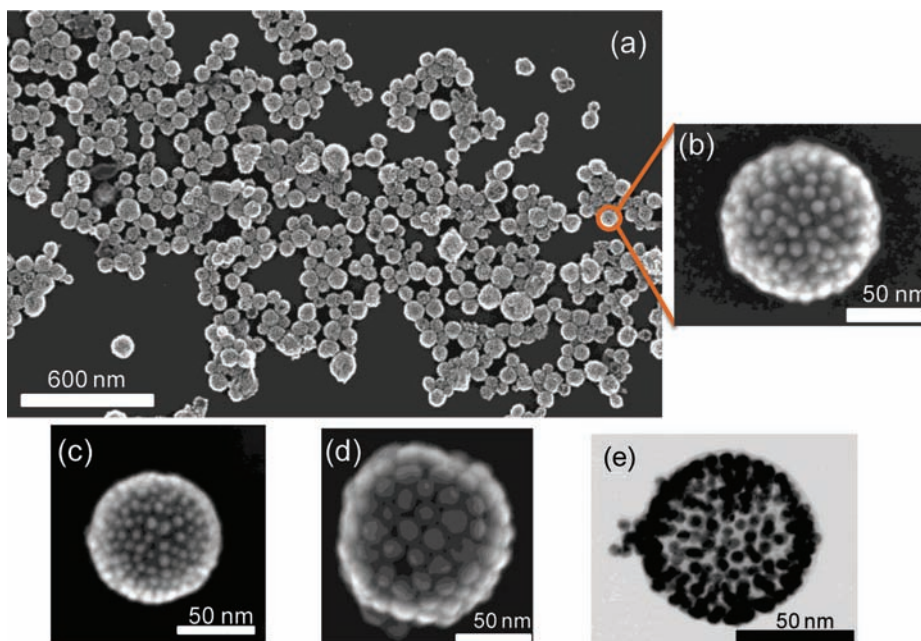


**Figure 1.** (a–d) SEM images of NP vesicles made from (a, b) 10, (c) 5, and (d) 20 nm SFL-AuNPs. (e) TEM image of an NP vesicle made from 10 nm SFL-AuNPs.

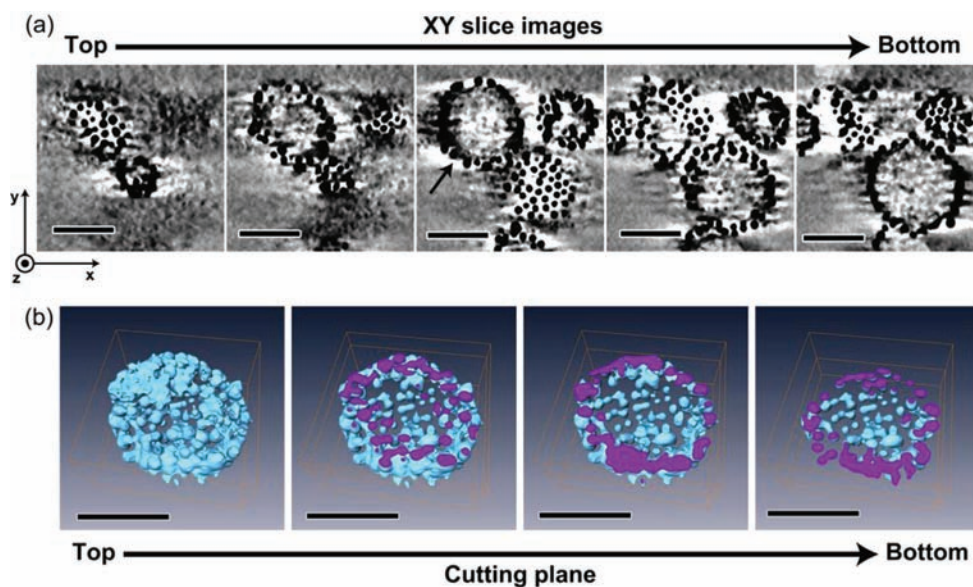


**Figure 2.** (a) Reconstructed images (XY plane) of NP vesicles embedded in epoxy resin. (b) 3D structures of NP vesicles as indicated by the black arrow in (a). Scale bars are 50 nm.

SFLs from 2 to 3 or 4. This increase did not affect the vesicular assemblies; however, SFLs without OEG or a fluorinated segment did not produce AuNP vesicular assemblies (Figure S3), indicating that both segments are essential for the formation of NP vesicles. Importantly, these NP vesicles could be observed only when the ligand exchange was carried out in THF. We examined many general solvents, such as H<sub>2</sub>O, methanol, butanol, ethyl acetate, acetone, toluene, dichloromethane, and hexane; however, no NP vesicle formation was observed. Thus, the solubility of the terminal OEG and FG segments in THF is an important factor in the NP assembly.

NMR spectroscopy is one of the most powerful methods for examining the structure of ligands immobilized on NPs.<sup>18</sup> Figure 3 shows the <sup>1</sup>H NMR spectra of free SFLs in methanol-*d*<sub>4</sub> and SFL-AuNPs in methanol-*d*<sub>4</sub> and THF-*d*<sub>8</sub>. The sharp, characteristic NMR spectrum (Figure 3b) indicates the unique molecular motion of SFLs linked to the AuNPs. The protons of the terminal OEG segment (peak f) were observed as sharp signals, whereas the protons adjacent to the FG segment (peak e) disappeared because of significant line broadening. This suggests that the OEG segments on AuNPs were directly accessible to the solvent with high flexibility, similar to those in the free-form SFLs in methanol. At the same time, the motion of the FG segments was significantly suppressed, as shown by the disappearance of peak e, indicating that the FG segments contribute to the bundle formation (Figure 3d). In THF, the SFL-AuNPs displayed a significantly broadened spectrum. Protons derived from both the OEG and FG segments were not detected, although the signal corresponding to the alkyl chain protons (peak c) was apparent, indicating that the motion of the terminal OEG segment and the FG segment was drastically suppressed in THF. We propose that the solvophobic feature of the FG segment is the main driving force behind the NP assembly (Figure 3d). In fact, fluorinated compounds are known to demonstrate a solvophobic feature.<sup>19</sup> In addition, especially in THF, OEG aggregation may also assist vesicle formation. PEG derivatives tend to aggregate in THF.<sup>20</sup> To stabilize the NP vesicles, electrostatic repulsion between the NPs is thought to be important.<sup>21</sup> SFL-coated AuNPs

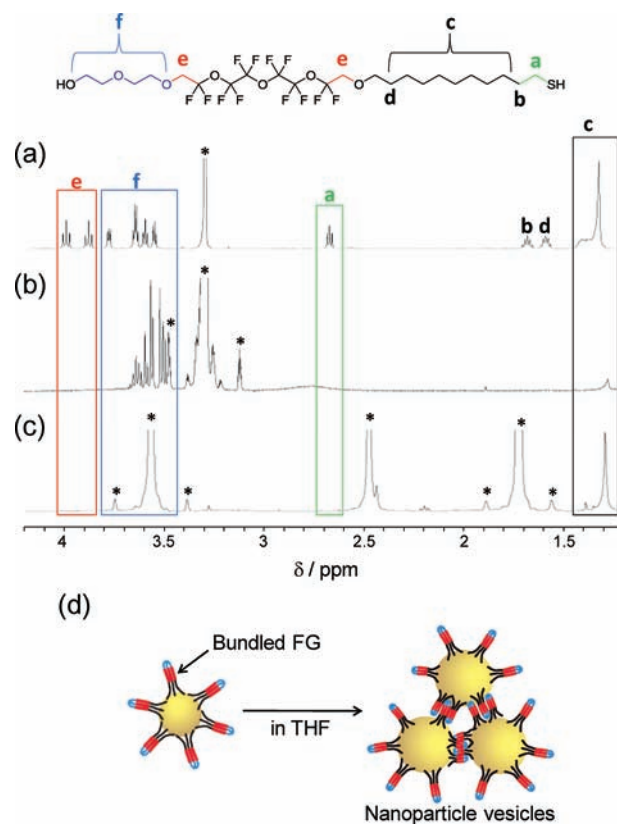


**Figure 3.** <sup>1</sup>H NMR spectra of (a) free SFLs in methanol-*d*<sub>4</sub>, (b) SFL-AuNPs in methanol-*d*<sub>4</sub>, and (c) SFL-AuNPs in THF-*d*<sub>8</sub>. \* represents signals derived from solvents. (d) Schematic presentation of SFLs on AuNPs in THF.

showed a  $\zeta$  potential of  $-7.8$  mV. This electrostatic repulsion would stabilize monolayer formation by preventing layering of the NPs. The sharpness of the alkyl chain peak c in THF means that the alkyl chains are partially exposed to THF, which is a good solvent for alkyl chains. This solubility of the alkyl segment is also thought to contribute to the stable dispersibility

of the NP vesicles in THF. In addition to  $^1\text{H}$  NMR measurements,  $^{19}\text{F}$  NMR measurements were also performed to analyze the FG segments directly. As in  $^1\text{H}$  NMR spectra, fluorine signals derived from free SFLs were clearly observed in THF- $d_8$  and methanol- $d_4$  (data not shown), whereas those of SFL-AuNPs were not detected in either solvent, supporting our assumption that the solvophobic feature of the FG segments contributes to the formation of the NP vesicles.

Interestingly, the vesicle structures formed in THF were maintained even after dispersion into different solvents, including nonpolar ( $\text{CH}_2\text{Cl}_2$ , ethyl acetate) and polar (butanol) solvents (Figure S4), indicating the stability of the spherical morphology. Using Monte Carlo simulations, Kegel and co-workers demonstrated that a hollow shell composed of individual NPs made on a template is intrinsically stable even after removal of the template.<sup>21</sup> Our data appear to support the results of these simulations and the general utility of NP vesicles in various organic solvents. In water, however, the NP vesicles were not dispersed but rather were aggregated.

SERS enhancement is one of the attractive applications for NP vesicles, as dispersed vesicles are suitable for direct SERS detection of analytes in solution. In the presence of the NP vesicles, SERS signals from crystal violet were clearly observed, whereas in the case of dispersed AuNPs, no signals were observed (Figure S5), indicating that NP vesicles can act as a platform for Raman-based sensing in solutions.

In summary, we have found that AuNPs coated with semifluorinated OEG ligands efficiently provide sub-100 nm hollow NP assemblies in THF. The NP vesicles were SERS-active in THF. Our approach was based on the unique function of the fluorinated OEG region, which induces the bundling of ligand molecules on NPs. This approach using a single OEG derivative appears to be applicable to the construction of NP vesicles from various kinds of colloidal particles. We are currently exploring the chemical modification of AuNPs (such as cross-linking) in NP vesicles to be utilized as plasmon-active drug delivery carriers in aqueous solutions.

## ■ ASSOCIATED CONTENT

### ● Supporting Information

Experimental details and supporting figures. This material is available free of charge via the Internet at <http://pubs.acs.org>.

## ■ AUTHOR INFORMATION

### Corresponding Author

kniikura@poly.es.hokudai.ac.jp

### Notes

The authors declare no competing financial interest.

## ■ ACKNOWLEDGMENTS

This work was supported by JST-CREST and KAKENHI 22655050: Grant-in-Aid for Challenging Exploratory Research. A part of this work was conducted at Hokkaido Innovation through Nanotechnology Support (HINTS), supported by the "Nanotechnology Network JAPAN" Program of the Ministry of Education, Culture, Sports, Science and Technology (MEXT), Japan.

## ■ REFERENCES

(1) Nie, Z.; Petukhova, A.; Kumacheva, E. *Nat. Nanotechnol.* **2010**, *5*, 15.

(2) Jones, M. R.; Osberg, K. D.; Macfarlane, R. J.; Langille, M. R.; Mirkin, C. A. *Chem. Rev.* **2011**, *111*, 3736.

(3) Li, F.; Josephson, D. P.; Stein, A. *Angew. Chem., Int. Ed.* **2011**, *50*, 360.

(4) (a) Yang, X. C.; Samanta, B.; Agasti, S. S.; Jeong, Y.; Zhu, Z. J.; Rana, S.; Miranda, O. R.; Rotello, V. M. *Angew. Chem., Int. Ed.* **2011**, *50*, 477. (b) Sanson, C.; Diou, O.; Thévenot, J.; Ibarboure, E.; Soum, A.; Brulet, A.; Miraux, S.; Thiaudière, E.; Tan, S.; Brisson, A.; Dupuis, V.; Sandre, O.; Lecommandoux, S. *ACS Nano* **2011**, *5*, 1122.

(5) Yang, M.; Alvarez-Puebla, R.; Kim, H. S.; Aldeanueva-Potel, P.; Liz-Marzán, L. M.; Kotov, N. A. *Nano Lett.* **2010**, *10*, 4013.

(6) Cabral, H.; Matsumoto, Y.; Mizuno, K.; Chen, Q.; Murakami, M.; Kimura, M.; Terada, Y.; Kano, M. R.; Miyazono, K.; Uesaka, M.; Nishiyama, N.; Kataoka, K. *Nat. Nanotechnol.* **2011**, *6*, 815.

(7) Pickering, S. U. *J. Chem. Soc., Trans.* **1907**, *91*, 2001.

(8) (a) Dinsmore, A. D.; Hsu, M. F.; Nikolaidis, M. G.; Marquez, M.; Bausch, A. R.; Weitz, D. A. *Science* **2002**, *298*, 1006. (b) Saigal, T.; Dong, H.; Matyjaszewski, K.; Tilton, R. D. *Langmuir* **2010**, *26*, 15200. (c) Nie, Z.; Park, J. I.; Li, W.; Bon, S. A. F.; Kumacheva, E. *J. Am. Chem. Soc.* **2008**, *130*, 16508. (d) Thompson, K. L.; Armes, S. P.; Howse, J. R.; Ebbens, S.; Ahmad, I.; Zaidi, J. H.; York, D. W.; Burdiss, J. A. *Macromolecules* **2010**, *43*, 10466.

(9) Rasch, M. R.; Rossinyol, E.; Hueso, J. L.; Goodfellow, B. W.; Arbiol, J.; Korgel, B. A. *Nano Lett.* **2010**, *10*, 3733.

(10) (a) Song, C.; Zhao, G.; Zhang, P.; Rosi, N. L. *J. Am. Chem. Soc.* **2010**, *132*, 14033. (b) Hwang, L.; Zhao, G.; Zhang, P.; Rosi, N. L. *Small* **2011**, *7*, 1939.

(11) Cha, J. N.; Birkedal, H.; Euliss, L. E.; Bartl, M. H.; Wong, M. S.; Deming, T. J.; Stucky, G. D. *J. Am. Chem. Soc.* **2003**, *125*, 8285.

(12) Nie, Z.; Fava, D.; Kumacheva, E.; Zou, S.; Walker, G. C.; Rubinstein, M. *Nat. Mater.* **2007**, *6*, 609.

(13) Nikolic, M. S.; Olsson, C.; Salcher, A.; Kornowski, A.; Rank, A.; Schubert, R.; Fromsdorf, A.; Weller, H.; Forster, S. *Angew. Chem., Int. Ed.* **2009**, *48*, 2752.

(14) Song, J.; Cheng, L.; Liu, A.; Yin, J.; Kuang, M.; Duan, H. *J. Am. Chem. Soc.* **2011**, *133*, 10760.

(15) Chen, C.-F.; Tzeng, S.-D.; Chen, H.-Y.; Lin, K.-J.; Gwo, S. *J. Am. Chem. Soc.* **2008**, *130*, 824.

(16) Luedtke, W. D.; Landman, U. *J. Phys. Chem. B* **1998**, *102*, 6566.

(17) (a) Jinnai, H.; Spontak, R. J. *Polymer* **2009**, *50*, 1067. (b) Jinnai, H.; Spontak, R. J.; Nishi, T. *Macromolecules* **2010**, *43*, 1675.

(18) Badia, A.; Singh, S.; Demers, L.; Cuccia, L.; Brown, G. R.; Lennox, R. B. *Chem.—Eur. J.* **1996**, *2*, 359.

(19) Ishikawa, Y.; Kuwahara, H.; Kunitake, T. *J. Am. Chem. Soc.* **2004**, *116*, 5579.

(20) (a) Gitsov, I.; Fréchet, J. M. J. *J. Am. Chem. Soc.* **1996**, *118*, 3785. (b) Gitsov, I.; Wooley, K. L.; Fréchet, J. M. J. *Angew. Chem., Int. Ed. Engl.* **1992**, *31*, 1200.

(21) Mani, E.; Sanz, E.; Bolhuis, P. G.; Kegel, W. K. *J. Phys. Chem. C* **2010**, *114*, 7780.